Testing of pseudopotentials used in classical Car - Parrinello simulations

Testing of pseudopotentials used in classical Car–Parrinello simulations

Hartmut Löwen† and Irene D'Amico‡

Institut für Festkörperforschung, Forschungszentrum Jülich, D-52425 Jülich, Germany

Abstract. Recently a classical scheme of the Car–Parrinello method was proposed to simulate charged colloidal suspensions described by the highly asymmetric 'primitive model' of electrolytes. To make the simulations feasible one has to rely on a pseudopotential picture which smooths out the counterionic density profile near the macroionic surfaces. Using 'exact' Monte Carlo simulations of the same model with two macroions only, we critically test the validity of the pseudopotential construction. We find that the effective forces between the macroions and the counterion density fields are satisfactorily described by pseudopotential theory for strongly interacting macroions. However, for a configuration of nearly touching macroions, there are substantial deviations. Variants of linear screening theory lead to less satisfactory comparison with the Monte Carlo data than the '*ab initio*' calculations supplemented with the pseudopotential picture. Among all linear screening models, the Poisson–Boltzmann-cell model supplemented with a size correction is found to be the best description.

1. Introduction

The great challenge of condensed matter theory is to understand the macroscopic properties of a given material arising from the interactions between the microscopic particles, i.e. electrons and ions. The past ten years have seen a tremendous success in predicting such macroscopic quantities (such as the phase diagram) by so-called '*ab initio*' computer simulations. In particular, Car–Parrinello-type [1, 2] simulations were extremely helpful for predicting the structure and thermodynamics of metals and semiconductors. The key idea is to treat the quantum mechanical electrons within density functional theory and couple their density field then to the molecular dynamics of the classical ions. Subsequently, this method was also applied to pure classical systems, particularly charged colloidal suspensions [3, 4], where the role of the electrons is played by classical counterions. In this context, the basic microscopic interactions are modelled within the primitive model of strongly asymmetrical electrolytes involving both an excluded-volume contribution from the finite mesoscopic core of the charged colloidal particles and long-ranged Coulomb terms. The microscopic counterions are treated within density functional theory of an inhomogeneous plasma which is combined with the molecular dynamics of the oppositely charged macroions. Since, at least in principle, only the bare microscopic (or mesoscopic) interactions are entering into

---

† Also at: Institut für Theoretische Physik II, Heinrich-Heine-Universität Düsseldorf, Universitätsstraße 1, D-40225 Düsseldorf, Germany.
‡ Present address: Department of Physics and Astronomy, University of Missouri–Columbia, Columbia, MO 65211, USA.

the model, one may call these Car–Parrinello methods '*ab initio*' calculations meaning that one starts from the very beginning, i.e. the microscopic level of the interactions.

However, if one really wants to simulate an actual material, these methods are strictly speaking not '*ab initio*' since most frequently one has to invoke additional (sometimes rather technical) assumptions and approximations. One principal problem is that the exact density functional is not known, either for the classical plasma or for the interacting electron gas. So one would do better to speak of density functional computer simulations. One can overcome this problem by arguing that the spatial modulation of the electron (or plasma) density is weak, justifying the local density approximation for the free-energy functional [5]. A second more practical problem, also related to the first one, is the behaviour of this density field near the ionic (or macroionic) cores. Typically, the wavefunction of valence electrons is strongly oscillating inside the ion cores. In the colloidal context, this problem is even more severe since the density field piles up near the macroionic surface due to the strong Coulomb attraction and then is exactly zero inside the impenetrable macroionic spheres. This immediately implies a high resolution of the density field in real space which makes the simulation quite expensive since one has to include many grid points in real space or wave-vectors in reciprocal-space sums. In order to overcome this problem one has to rely on the validity of *pseudopotentials* [6]. The key idea of the pseudopotential picture is to introduce a fictitious ion–electron (or macroion–counterion) interaction that leads to the same electronic wavefunction (or counterion density field) outside the ionic cores. Hence two basic requirements have to be fulfilled by any pseudopotential:

(i) it has to be *norm-conserving,* i.e. the wavefunction (or density field) has to be identical outside the cores [7]; and

(ii) it has to be *transferable,* i.e. the norm-conserving property has to be fulfilled in any typical ionic configuration [8].

In the electronic context, a lot of experience has accumulated during the past three decades on how to construct and use pseudopotentials for many different atomic systems; see e.g. [6]. These potentials were tested in great detail [9]. Much less is known as regards the validity of classical pseudopotentials. In this paper we compare exact results for the effective force between two macroions gained by Monte Carlo simulation of the primitive model with the '*ab initio*' results which rely on the validity of the pseudopotential picture. For typical configurations, i.e. for those macroionic configurations which have a reasonable statistical weight, the results are in fact very close, while there are increasing deviations for nearly touching macroions and for very high macroion packing fractions. This means that the '*ab initio*' simulations can in general be trusted if one has a calculation of the pair structure and thermodynamics in mind. Rare events such as coagulation, however, cannot be correctly described by pseudopotential theory.

The paper is organized as follows. In section 2 we describe the primitive model for the interactions. Then we give the definition of the effective macroionic forces in section 3. After having discussed the different theoretical approaches in detail in section 4, we present our results in section 5. The final section, section 6, is devoted to conclusions and the outlook.

2. The primitive model

The physical system that we have in mind is that of charged mesoscopic colloidal macroions suspended in a microscopic fluid together with their microscopic counterions. The macroions carry a charge Ze that is normally two or three orders of magnitude larger than the charge

$-qe$ of the monovalent or divalent microscopic counterions. Here, e denotes the elementary charge. We consider N_m macroions with diameter $\sigma \equiv 2R$ confined in a volume V corresponding to a finite number density $\rho_m = N_m/V$ at a temperature T. The macroion density can conveniently be expressed in terms of their volume fraction $\phi_m = \pi\rho_m\sigma^3/6$. The counterions possess a number density which is determined by global charge neutrality to be

$$\rho_c = Z\rho_m/q. \tag{1}$$

Within the 'primitive model' the solvent solely enters via its dielectric constant ϵ reducing the Coulomb interaction between the charged species. One assumes the following pair interaction potentials $V_{mm}(r)$, $V_{mc}(r)$, $V_{cc}(r)$ between macroions and counterions, r denoting the corresponding interparticle distance:

$$V_{mm}(r) = \begin{cases} \infty & \text{for } r < \sigma \\ \dfrac{Z^2e^2}{\epsilon r} & \text{for } r \geqslant \sigma \end{cases} \tag{2}$$

$$V_{mc}(r) = \begin{cases} \infty & \text{for } r < \sigma/2 \\ -\dfrac{Zqe^2}{\epsilon r} & \text{for } r \geqslant \sigma/2 \end{cases} \tag{3}$$

$$V_{cc}(r) = \frac{q^2e^2}{\epsilon r}. \tag{4}$$

The counterions represent a one-component classical plasma (OCP) with the Coulomb repulsion (4) containing a further length scale, the so-called Bjerrum length

$$\lambda_B = e^2/\epsilon k_B T$$

where k_B is Boltzmann's constant. For water ($\epsilon = 78.0$) at room temperature ($T = 300$ K), $\lambda_B = 7.2$ Å.

For high charge asymmetry corresponding to typical samples of charged suspensions, the 'primitive model' cannot be solved for large N_m by direct computer simulation on present-day computers. Within classical Car–Parrinello-type (so-called '*ab initio*') simulations, however, this becomes feasible with the price of the additional pseudopotential approximation. The key idea of this paper is to treat a special configuration of only two macroions ($N_m = 2$) which are placed along the room diagonal of a cubic box with periodic boundary conditions. The macroion centres are separated by a distance r and are surrounded by their periodic images. The length L of the cube as determined by the macroion density is $L = (2/\rho_m)^{1/3}$; see figure 1. This corresponds to a configuration of a bcc crystal distorted in the (111) direction. One should bear in mind that due to the periodic boundary conditions and image particles this is a many-body (though highly correlated) macroionic configuration. In such a small system, one cannot calculate the structural correlation or the thermodynamics due to the finite system size. However, one can extract the distance-resolved effective macroion forces and the density field of the counterions. For $N_m = 2$, a direct Monte Carlo simulation of the primitive model is possible [10]. Comparing the effective macroion forces with the '*ab initio*' data, one can hence test the validity of the pseudopotential approximation inherent in any '*ab initio*' simulation.

3. Effective macroion forces

Let us now give the statistical definitions of the *effective macroion forces*. They clearly contain two parts, one stemming from the direct Coulomb repulsion between the macroions
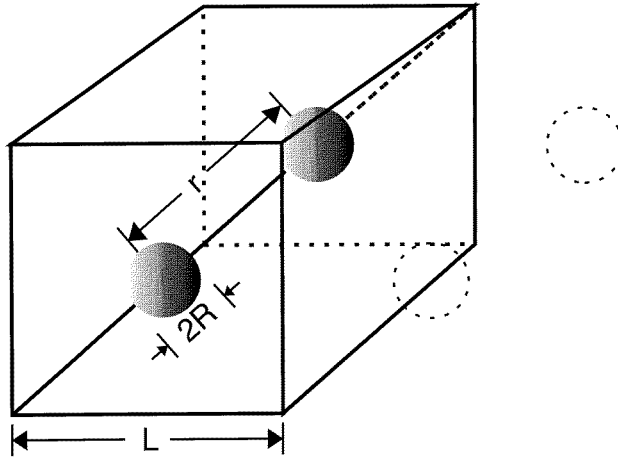
Figure 1. The configuration of two macroions (dark spheres) of radius R and central distance r studied in the paper. They are placed along the room diagonal of a cube of length L. The size of the cube is determined by the macroion density. Due to the periodic boundary conditions, all periodic images of the macroions are also taken into account. Two of these image charges are shown as broken circles. The counterions which are also periodically repeated are not shown.

(2) and the other from the macroion–counterion interaction (3). This implies that the force $\boldsymbol{F}_i$ acting on the ith macroion located at $\boldsymbol{R}_i$ can be written as

$$\boldsymbol{F}_i = \boldsymbol{F}_i^{(m)} + \boldsymbol{F}_i^{(c)} \tag{5}$$

where the direct macroionic part $\boldsymbol{F}_i^{(m)}$ is the pairwise Coulomb repulsion:

$$\boldsymbol{F}_i^{(m)} = -\boldsymbol{\nabla}_{\boldsymbol{R}_i} \sum_{j=1; j\neq i}^{N_m} V_{mm}(|\boldsymbol{R}_i - \boldsymbol{R}_j|) \tag{6}$$

$\{\boldsymbol{R}_j; j = 1, \ldots, N_m\}$ being the given macroion positions. The second contribution to the total effective force, $\boldsymbol{F}_i^{(c)}$, is the canonically counterion-averaged force from the macroion–counterion interaction (3):

$$\boldsymbol{F}_i^{(c)} = -\left\langle \sum_{j=1}^{N_c} \boldsymbol{\nabla}_{\boldsymbol{R}_i} V_{mc}(|\boldsymbol{R}_i - \boldsymbol{r}_j|) \right\rangle_c. \tag{7}$$

Here, $\{\boldsymbol{r}_j; j = 1, \ldots, N_c\}$ are the counterion positions and the canonical average $\langle \cdots \rangle_c$ over an $\{\boldsymbol{r}_j\}$-dependent quantity $\mathcal{A}$ is defined via the classical trace

$$\langle \mathcal{A}(\{\boldsymbol{r}_k\}) \rangle_c = \frac{1}{\mathcal{Z}} \frac{1}{N_c!} \frac{1}{\Lambda^{3N_c}} \int_V \mathrm{d}^3 r_1 \cdots \int_V \mathrm{d}^3 r_{N_c} \, \mathcal{A}(\{\boldsymbol{r}_k\}) \exp\left[-\frac{V_c}{k_B T} \right] \tag{8}$$

where V is the system volume, Λ is the de Broglie thermal wavelength of the counterions and

$$V_c = \sum_{n=1}^{N_m} \sum_{j=1}^{N_c} V_{mc}(|\boldsymbol{R}_n - \boldsymbol{r}_j|) + \frac{1}{2} \sum_{i,j=1; i\neq j}^{N_c} V_{cc}(|\boldsymbol{r}_i - \boldsymbol{r}_j|) \tag{9}$$

is the total counterionic part of the potential energy. Furthermore, the classical partition function

$$\mathcal{Z} = \frac{1}{N_c!} \frac{1}{\Lambda^{3N_c}} \int_V d^3r_1 \cdots \int_V d^3r_{N_c} \exp\left[-\frac{V_c}{k_B T}\right] \tag{10}$$

guarantees the correct normalization $\langle 1 \rangle_c = 1$.

An alternative expression for the counterion-induced forces $\boldsymbol{F}_i^{(c)}$ can be obtained by using the inhomogeneous *equilibrium counterion density profile* in the field of fixed macroions which is defined via

$$\rho_c(\boldsymbol{r}; \{\boldsymbol{R}_j\}) = \left\langle \sum_{n=1}^{N_c} \delta(\boldsymbol{r} - \boldsymbol{r}_n) \right\rangle_c. \tag{11}$$

Then $\boldsymbol{F}_i^{(c)}$ can be rewritten as

$$\boldsymbol{F}_i^{(c)}(\{\boldsymbol{R}_j\}) = -\int_V d^3r \; \rho_c(\boldsymbol{r}; \{\boldsymbol{R}_j\}) \, \boldsymbol{\nabla}_{\boldsymbol{R}_i} V_{mc}(|\boldsymbol{r} - \boldsymbol{R}_i|). \tag{12}$$

Denoting with $\boldsymbol{R}_1$ and $\boldsymbol{R}_2$ the positions of the two macroions in our case, we have $\boldsymbol{F}_1 = -\boldsymbol{F}_2$ and the total effective force depends only on the macroion distance $r = |\boldsymbol{R}_2 - \boldsymbol{R}_1|$. From symmetry considerations, the direction of $\boldsymbol{F}_1$ is along the room diagonal, i.e. parallel to $\boldsymbol{R}_1 - \boldsymbol{R}_2$. We therefore consider only the magnitude of the force projecting it onto the room diagonal

$$F(r) = \boldsymbol{F}_1(r) \cdot (\boldsymbol{R}_1 - \boldsymbol{R}_2)/r \tag{13}$$

which is the key quantity of this paper. Clearly, $F(r)$ vanishes in a symmetric configuration of a bcc crystal when the two particles are separated by a distance $r \equiv r_0 = (\sqrt{3}/2)L$. The force $F(r)$ will be linear in r around $r = r_0$. In general, we expect repulsive forces, i.e. $F(r) > 0$. Near contact, $r \gtrsim 2R$, the magnitude of F governs colloidal coagulation if an additional van der Waals interaction is present.

The force $F(r)$ is a rather sensitive quantity which gives direct insight into the effective interactions. For instance, pair correlations are much more insensitive to the microscopic interactions.

A direct interpretation of $F(r)$ in terms of a bare effective macroionic pair interaction is invalidated somewhat by the fact that all of the periodic images may also contribute. This implies that $F(r)$ is not the direct effective pair potential between two macroions. For short-ranged effective potentials and close separations r, however, these contributions are small. On the other hand, if an effective pair potential $U(r)$ (e.g. obtained within linear screening theory) is given, one can calculate the effective forces resulting from this potential in the presence of the periodic images of the macroions and compare with the exact Monte Carlo data. In fact, there are different recipes for obtaining such a pair potential from linear screening. The actual form is always a Yukawa expression of the type

$$U_{(i)}(r) = \frac{Z_{(i)}^{*\,2} e^2}{\epsilon r} \exp(-\kappa_{(i)} r) \tag{14}$$

but the prefactor—or alternatively the effective macroion charge $Z_{(i)}^*$—and the screening constant $\kappa_{(i)}$ differ in different models labelled by (i). This will be discussed in more detail in the next section. The effective force is then given by

$$F(r) \approx \left| \boldsymbol{\nabla}_{\boldsymbol{R}_1} \sum_{\boldsymbol{n}} U_{(i)}(|\boldsymbol{R}_1 - r\boldsymbol{e} - \boldsymbol{R}_{\boldsymbol{n}}^{(0)}|) \right| \tag{15}$$

where $\boldsymbol{R}_{\boldsymbol{n}}^{(0)} = (2/\sqrt{3})r_0\boldsymbol{n}$ are all cubic lattice vectors labelled by $\boldsymbol{n} \equiv (n_x, n_y, n_z)$ and $\boldsymbol{e}$ is a unit vector along the room diagonal.

4. Different theoretical approaches to the effective forces

4.1. Monte Carlo simulation

We used the standard Monte Carlo scheme [11] treating the long-ranged Coulomb forces using Ewald sums. We start with an arbitrary counterion configuration which does not penetrate into the two fixed macroion cores. Typically 2×10^4 Monte Carlo steps per counterion are used to equilibrate the counterions and then the canonical average (7) is taken for 4×10^4 Monte Carlo steps per particle. We also obtained the inhomogeneous counterion equilibrium density along the room diagonal by directly exploiting its definition, equation (11).

4.2. 'Ab initio' simulation and the pseudopotential construction

In addition we have done 'ab initio' calculations according to reference [4], but now for two macroions in the configuration sketched in figure 1. They key quantity of this approach is the inhomogeneous equilibrium counterion density which is gained by minimizing the free-energy density functional in the external field of the fixed macroions. We have used the expression (12) to obtain the effective forces. The pseudopotential construction is done in the same way as described in reference [4]: in order to include the impenetrable macroion core approximatively, we make it penetrable such that the true potential $V_{mc}(r)$ in equation (3) is replaced by the 'pseudopotential'

$$V'_{mc}(r) = -\frac{Zqe^2}{\epsilon r} \, \text{erf}(r/R_c) \tag{16}$$

where R_c is chosen to be $\simeq R/2$. This leads to an extra, unphysical, counterion charge inside the cores, which must be compensated by increasing the macroion charge from Ze to $(Z + Z_m^*)e$. The permeability of the macroions leads to unwanted fluctuations of the counterion charge density inside the cores, and hence of the apparent macroion charge, which will strongly affect the static and dynamical properties of the macroion fluid. Therefore, in a second step of the pseudopotential construction, these fluctuations are efficiently damped by simultaneously assigning a severe free-energy handicap to the excess counterion charge inside the macroions; see reference [4] for details. The whole pseudopotential procedure should result in a 'norm-conserved' counterion density $\rho_c(\mathbf{r})$ which is smooth inside the macroion cores, but coincides with the physical density outside the cores. At the same time, the continuity of the pseudopotential construction which takes care of a stiff counterionic density profile *inside* the macroionic cores also suppresses an accumulation of counterions near the macroionic surfaces *outside* the cores.

The 'transferability' of this pseudopotential construction was hitherto only checked indirectly and *a posteriori*. It was shown that the actual counterion fluctuations inside the macroion core are indeed smaller than those outside the core [4]. However, the direct effect of the pseudopotential approximation on the effective macroion forces which govern the macroionic structural correlations was not investigated quantitatively in reference [4] and is the scope of the present paper.

4.3. Effective pairwise Yukawa models

Let us summarize four different Yukawa-like models for the effective pairwise interaction $U_{(i)}(r)$ of equation (14) ($i = 1, 2, 3, 4$).

(1) *DLVO theory.* In the traditional linear screening theory of Derjaguin, Landau, Verwey and Overbeek (DLVO) [12], which was derived for low macroion packing fraction, we have ($i \equiv 1$)

$$Z^*_{(1)} = Z \exp(\kappa_{(1)} R)/(1 + \kappa_{(1)} R) \tag{17}$$

which gives a size correction to the bare charge Z and

$$\kappa_{(1)} = \sqrt{\frac{4\pi q^2 e^2 \rho_c}{\epsilon k_B T}}. \tag{18}$$

(2) *MSA theory.* It is possible to solve the mean-spherical approximation (MSA) of the primitive model analytically [13]. In this picture ($i \equiv 2$) the effective macroionic interaction is again a Yukawa potential with an effective charge $Z^*_{(2)}$ which is larger than $Z^*_{(1)}$ while $\kappa_{(2)} \equiv \kappa_{(1)}$.

(3) *The Poisson–Boltzmann-cell (PBC) approach.* In this theory ($i \equiv 3$) one solves the nonlinear Poisson–Boltzmann equations in a spherical Wigner–Seitz cell centred around a single macroion [14]. The Wigner–Seitz radius is determined by the macroion density. The Poisson–Boltzmann equations are then linearized around a counterion density $\bar{\rho}_c$ which is determined self-consistently such that the mean counterion density of the linearized solution coincides with $\bar{\rho}_c$. Then

$$Z^*_{(3)} = q \bar{\rho}_c / \rho_m \tag{19}$$

is determined by global charge neutrality and

$$\kappa_{(3)} = \sqrt{\frac{4\pi q^2 e^2 \bar{\rho}_c}{\epsilon k_B T}}. \tag{20}$$

(4) *The modified Poisson–Boltzmann-cell (MPB) approach.* This approach ($i \equiv 4$) is similar to the former one [14]. The difference is that one takes the counterion density at the Wigner–Seitz cell boundary, $\tilde{\rho}_c$, from the solution of the Poisson–Boltzmann equations and linearizes these equation around $\tilde{\rho}_c$. Then one arrives at a result very similar to the PBC approach [15]. However, we take a size correction similar to (17) into account; see again [15]. Hence we get

$$Z^*_{(4)} = q \frac{\tilde{\rho}_c}{\rho_m} \frac{\exp(\kappa_{(4)} R)}{1 + \kappa_{(4)} R} \tag{21}$$

and

$$\kappa_{(4)} = \sqrt{\frac{4\pi q^2 e^2 \tilde{\rho}_c}{\epsilon k_B T}}. \tag{22}$$

5. Results

We have investigated three parameter combinations which were used in runs of '*ab initio*' calculations (runs A, B, and C) [4]. They are given in table 1. The dielectric constant of the solvent was fixed to be $\epsilon = 78$, the macroion radius was $R = \sigma/2 = 53$ nm, and the temperature was 300 K. In order to demonstrate the typical range of macroion distances r which have a reasonable statistical weight we have shown the '*ab initio*' data from reference [4] for the pair correlation function $g(r)$ in figure 2. If $g(r)$ is practically zero, then the probability of finding two macroions with such a distance is very small.
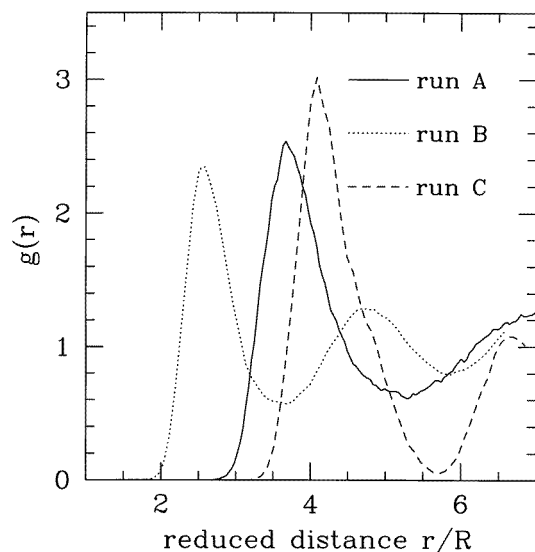
Figure 2. Macroion–macroion pair correlation functions $g(r)$ versus reduced distance r/R as obtained from '*ab initio*' simulations for the three different runs A, B, and C studied in this paper. From reference [4].

Table 1. Parameters for the three different runs A, B, C: the bare charge Z, macroion packing fraction ϕ_m, as well as the data for the screened Coulomb reference pairwise potentials: the effective charge $Z^*_{(i)}$ for model (i) ($i = 1, 2, 3, 4$) and the corresponding Debye screening parameter $\kappa_{(i)}R$ ($\kappa_{(1)} \equiv \kappa_{(2)}$).

Run	Z	ϕ_m	$Z^*_{(1)}$	$Z^*_{(2)}$	$Z^*_{(3)}$	$Z^*_{(4)}$	$\kappa_{(1)}R$	$\kappa_{(3)}R$	$\kappa_{(4)}R$
A	200	0.1	259	296	194	245	0.90	0.99	0.866
B	100	0.3	142	189	97.8	157	1.10	1.09	1.27
C	300	0.08	404	462	284	355	0.98	0.96	0.89

Using the different theoretical approaches discussed in the previous section, we have calculated the distance-resolved effective macroion forces $F(r)$. The results for the three parameter combinations (runs A, B, and C) are given in figures 3–5. Note that the parameters used for the four different Yukawa models are also given in table 1. We can draw the following conclusions.

(i) Apart from the PBC approach which is not corrected for the finite macroion size, all Yukawa models and also the '*ab initio*' approach produce forces that are *systematically too high*. This is expected for the following reasons. The linear response theory on the Debye–Hückel level gives a reduced counterion screening as compared to the nonlinear theory on the Poisson–Boltzmann level since the free energy per counterion is overestimated in the linear theory [4]. Extending the theory to a local density approximation (LDA) the counterion screening becomes again more effective [16] such that even overscreening (attraction) between plates has been found for extreme counterionic correlations. Here extreme counterion correlations of course only occur if the counterions themselves are strongly coupled. The Monte Carlo simulations also include fluctuations which give rise
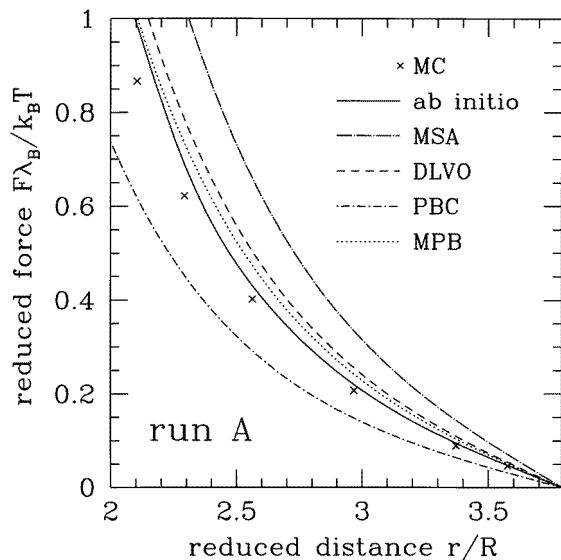
Figure 3. Effective macroion force F in units of $k_B T/\lambda_B$ versus reduced distance r/R for run A. The crosses are our Monte Carlo data. The statistical error is smaller than the cross size. Furthermore the '*ab initio*' data are given as well as those from the four different Yukawa models.
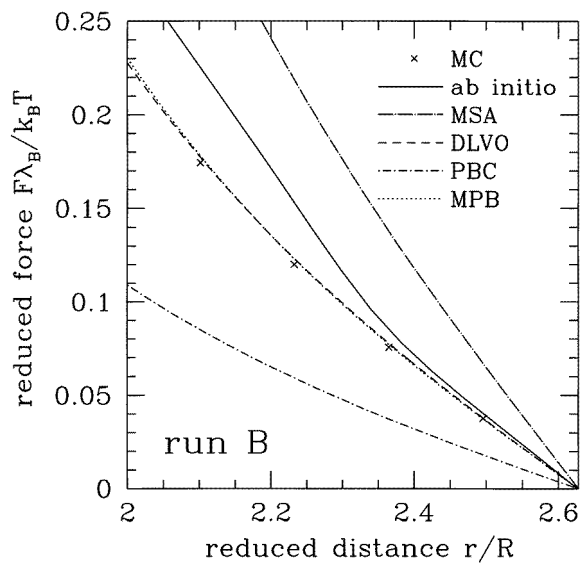

Figure 4. As figure 3, but now for run B.

to an additional attractive part to the total force. These fluctuations of the Stern layer are ignored in the mean-field-like density functional approach. Hence our results are consistent with the following sequence: the Debye–Hückel theory with size corrections produces stronger repulsions than the Poisson–Boltzmann theory which in turn produces
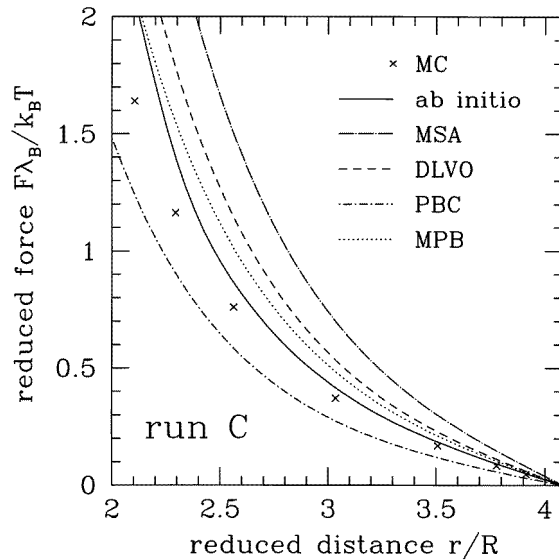
Figure 5. As figure 4, but now for run C.

stronger repulsions than the superior local density approximation. Finally the LDA again overestimates the forces since fluctuation-induced attractions (see e.g. [17] for a discussion) are not included here.

We finally remark that both of the Poisson–Boltzmann approaches discussed previously (namely PBC and MPB) are basically linear screening theories with parameters obtained from nonlinear screening theories. So they are somewhat in between the linear Debye–Hückel level and the full nonlinear Poisson–Boltzmann level.

Table 2. The gradient of the force near the perfect-lattice positions, $-\mathrm{d}F(r)/\mathrm{d}r|_{r=r_0}$ (in units of k_BT/R^2), for the three different runs and all of the different theoretical approaches.

Run	MC	*ab initio*	DLVO	MSA	PBC	MPB
A	15.5 ± 1.5	16.3	18.35	24.00	10.69	17.49
B	20 ± 2	22.8	21.04	37.25	10.09	20.76
C	20 ± 2	22.3	26.43	34.55	13.64	24.59

(ii) The '*ab initio*' data fit the Monte Carlo data well near $r = r_0$. This is explicitly demonstrated in table 2 where we have shown the gradient of the force $-\mathrm{d}F(r)/\mathrm{d}r$ evaluated at $r = r_0$. This quantity governs the energy scales as well as the dynamical properties of a harmonic solid. In the crystalline phase or for strongly interacting fluids (like run A and C), it is merely this quantity which determines the structural correlations as embodied in $g(r)$. From the data of table 2 we conclude that the '*ab initio*' results for the gradient are better than any Yukawa results for all of the three runs except for run B where the MPB model is slightly better. However, for closer macroionic separations r, the '*ab initio*' results deviate strongly from the Monte Carlo data. This is also expected since due to the pseudopotential construction accumulations of the counterions near the macroionic surfaces are suppressed which leads to a stronger repulsion. Such small distances do not bear any
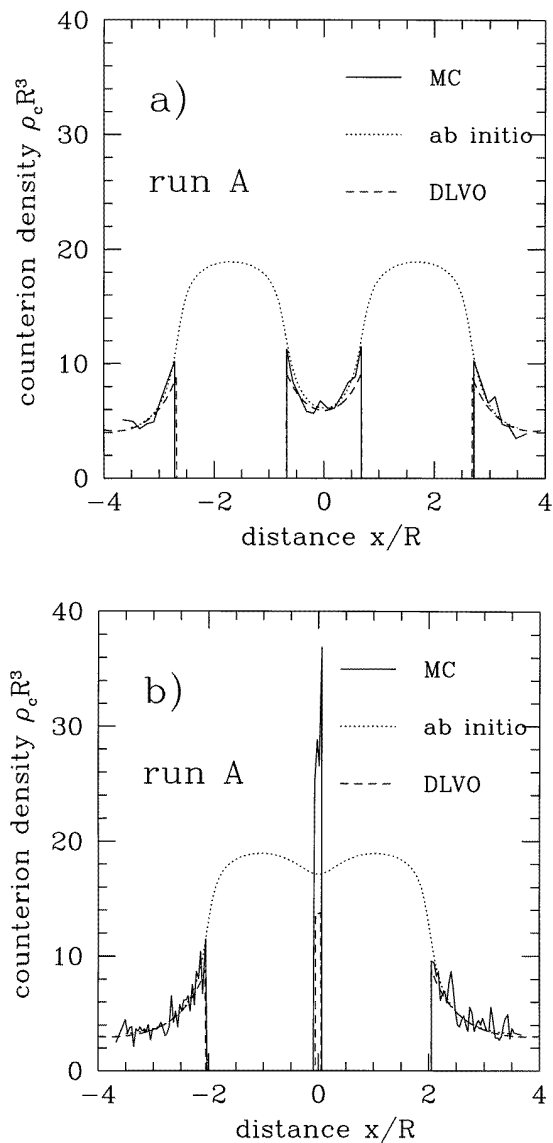
Figure 6. Counterion equilibrium density ρ_c in units of $1/R^3$ along a one-dimensional cut through the macroion centres. The x-coordinate is such that the origin coincides with the common centre of mass of the two macroions. The parameters are those for run A. Data for $\rho_c(x)$ are shown for two different macroion distances: (a) $r = 250\lambda_B$ and (b) $r = 156\lambda_B$. The solid lines are the Monte Carlo data, and the dotted lines are results from an '*ab initio*' simulation. Inside the macroionic cores the counterion does not vanish in the '*ab initio*' approach due to the pseudopotential picture. The dashed lines are obtained from DLVO theory. For the sake of clarity we set the DLVO density to be zero inside the macroionic cores.

statistical weight for run A and C (see again figure 2) but are important for run B. We thus conclude that the pseudopotential picture works well for strong coupling but fails in situations where the macroions approach each other. This immediately implies that the
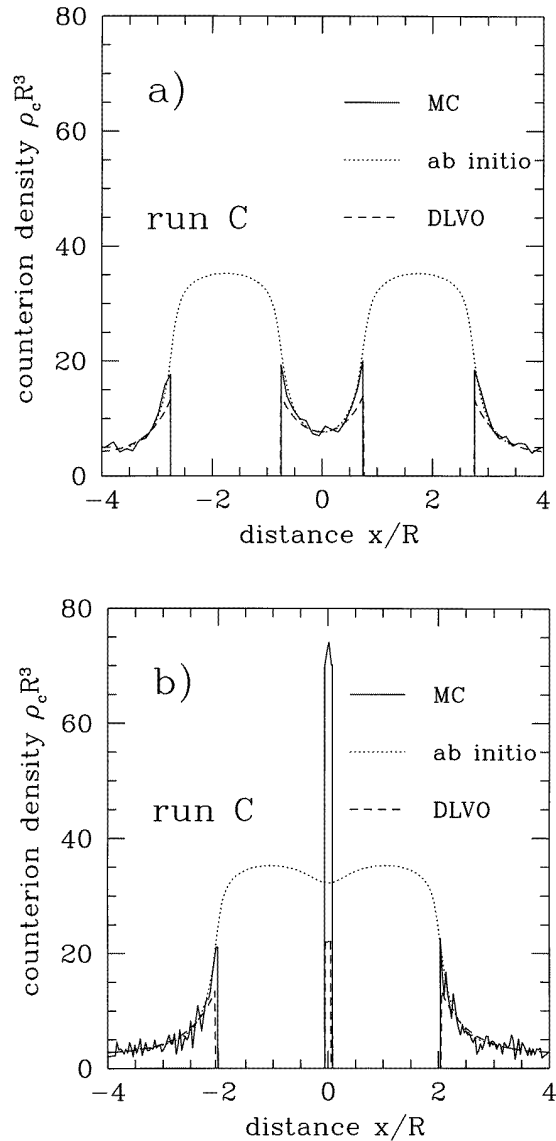
Figure 7. As figure 6, but now for run C. The two macroion distances are now (a) $r = 260\lambda_B$ and (b) $r = 156\lambda_B$.

pseudopotential construction is not valid if one has a calculation of the coagulation rate in mind [18, 19] which depends sensitively to the height of the energy barrier in the effective pair potential between two colloidal macroions.

(iii) Qualitatively the results for the Yukawa models are in agreement with the discussion in reference [4]. The MSA theory overestimates the forces while the PBC model underestimates the forces. DLVO theory works for weak coupling (as for run B) but fails for larger coupling (as for run A and C). The best overall agreement is achieved with the size-corrected Poisson–Boltzmann-cell approach MPB. This is consistent with the conclusions

of reference [15] where experimental data for self-diffusion could be fitted best within this Yukawa model.

Finally we have compared the counterion equilibrium density fields along a one-dimensional cut through the centres of the two macroions. In the '*ab initio*' approach, this is the central quantity obtained by minimizing the free-energy density functional. The Monte Carlo data still bear a considerable error since they were obtained by averaging over a small tube around this one-dimensional cut. Note that the MC data are not symmetrized around $x = 0$. The overall integral of this quantity is fixed by global charge neutrality. Hence it is less sensitive than the macroionic forces. Observing the comparison between the '*ab initio*' and the Monte Carlo data in figures 6 and 7, one reaches the same conclusion as before: if the macroions are well separated, then the results practically coincide. For nearly touching macroions, the counterion density in between the macroions is drastically reduced due to the stiffening process in the pseudopotential construction. This, of course, leads to the overestimation of the macroionic forces discussed previously.

While most of the linear screening theories do not predict the counterion density fields directly, the DLVO approach can be used to extract a counterionic density distribution around the macroions. In DLVO theory the counterion equilibrium density consists of a linear superposition of Yukawa orbitals [4]:

$$\rho_c(\boldsymbol{r}; \{\boldsymbol{R}_j\}) \approx \sum_{i=1}^{N_m} \frac{Z^*_{(1)}}{q} \frac{\kappa^2_{(1)}}{4\pi} \frac{\exp(-\kappa_{(1)}|\boldsymbol{r} - \boldsymbol{R}_i|)}{|\boldsymbol{r} - \boldsymbol{R}_i|} \qquad (23)$$

where the sum is over all macroions including all of their periodic images. We have also shown the DLVO result for the counterion density field in figures 6 and 7. The deviations with respect to the MC data are more severe than in the '*ab initio*' calculations. In particular, already for large macroion separations, the contact counterion density near the macroionic surfaces is underestimated by DLVO theory. For nearly touching macroions, the counterion density in between is even more underestimated than in the pseudopotential picture. This in turn explains again why the *ab initio* forces are smaller than the DLVO forces.

6. Summary and outlook

To summarize: we have presented 'exact' Monte Carlo results for the distance-resolved effective forces between two macroions in a many-body configuration. Testing the pseudopotential approach against these data, we found that it is justified in a strongly interacting system while there are substantial deviations for a configuration of nearly touching macroions.

One immediate consequence of our results is that it does not help to improve the density functional itself if one wants to improve the quality of '*ab initio*' simulations. In fact one knows better functionals of the inhomogeneous plasma than the LDA [20, 21] which could be used in '*ab initio*' approaches. However, the pseudopotential construction is the most important limitation and approximation. As it was used in reference [4], the pseudopotential construction is only possible for a local density approximation.

Looking forward, let us discuss further generalizations and limitations of the pseudopotential picture. First, it was used also for a situation of added salt ions in reference [22]. Here the counterion–macroion interaction was treated differently to the coion–macroion interaction. It is less clear how to generalize the pseudopotential construction to situations away from the bulk, as for macroions confined between charged plates [23, 24]

or in a gravitational field [25]. While a pseudopotential approach could be taken for rod-like charged colloid particles [26] it is not obvious how to deal with binary (or charge-polydisperse) mixtures of charged colloids [27]. These situations are challenging problems for the future.

Acknowledgments

References

[1] Car R and Parrinello M 1985 *Phys. Rev. Lett.* **55** 2471
[2] Remler D K and Madden P A 1990 *Mol. Phys.* **70** 921
[3] Löwen, Madden P A and Hansen J-P 1992 *Phys. Rev. Lett.* **68** 1081
[4] Löwen, Hansen J-P and Madden P A 1993 *J. Chem. Phys.* **98** 3275
[5] For a review, see
    Löwen H 1994 *Phys. Rep.* **237** 249
[6] See, e.g.,
    Bachelet G B, Hamann D R and Schlüter M 1982 *Phys. Rev.* B **26** 4199
[7] See, e.g.,
    Stokbro K 1996 *Phys. Rev.* B **53** 6869
[8] See, e.g.,
    Nogueira F, Fiolhais C, He J S, Perdew J P and Rubio A 1996 *J. Phys.: Condens. Matter* **8** 287
[9] See, e.g.,
    Milman V and Lee M H 1996 *J. Phys. Chem.* **100** 6093
[10] D'Amico I and Löwen H 1997 *Physica* A **237** 25
[11] See, e.g.,
    Allen M P and Tildesley D J 1989 *Computer Simulation of Liquids* (Oxford: Clarendon)
[12] Derjaguin B V and Landau L D 1941 *Acta Physicochim. USSR* **14** 633
    Verwey E J W and Overbeek J T G 1948 *Theory of the Stability of Lyophobic Colloids* (Amsterdam: Elsevier)
[13] Belloni L 1986 *J. Chem. Phys.* **85** 519
    Belloni L 1988 *J. Chem. Phys.* **88** 5143
[14] Alexander S, Chaikin P M, Grant P, Morales G J, Pincus P and Hone D 1984 *J. Chem. Phys.* **80** 5776
[15] Bitzer F, Palberg T, Löwen H, Simon R and Leiderer P 1994 *Phys. Rev.* E **50** 2821
[16] Stevens M and Robbins M O 1990 *Europhys. Lett.* **12** 81
[17] Schmitz K S 1990 *Dynamic Light Scattering by Macromolecules* (San Diego, CA: Academic) p 284
[18] Russel W B, Saville D A and Schowalter W R 1989 *Colloidal Dispersions* (Cambridge: Cambridge University Press)
[19] Sauer S and Löwen H 1996 *J. Phys.: Condens. Matter* **8** L803
[20] Groot R D 1988 *Phys. Rev.* A **37** 3456
[21] Rosenfeld Y 1993 *J. Chem. Phys.* **98** 8126
[22] Löwen H and Kramposthuber G 1993 *Europhys. Lett.* **23** 673
[23] See, e.g.,
    Kepler G M and Fraden S 1994 *Phys. Rev. Lett.* **73** 356
[24] Larsen A E and Grier D G 1997 *Nature* **385** 230
[25] See, e.g.,
    Biben T, Hansen J-P and Barrat J L 1993 *J. Phys. Chem.* **98** 7330
    Piazza R, Bellini T and Degiorgio V 1993 *Phys. Rev. Lett.* **71** 4267
[26] Löwen H 1994 *Phys. Rev. Lett.* **72** 424
    Löwen H 1994 *J. Phys. Chem.* **100** 6738
[27] See, e.g.,
    Mendez-Alcaraz J M, D'Aguanno B and Klein R 1991 *Physica* A **178** 421
    Meller A and Stavans J 1992 *Phys. Rev. Lett.* **68** 3646
    Sanyal S and Sood A K 1995 *Phys. Rev.* E **52** 4154